Nuclear Science and Techniques **22** (2011) 224–229

Influence factors of two dimensional position map on photomultiplier detector block designed by quadrant sharing technique

WEI Qingyang WANG Shi* Ma Tianyu MA Fei DAI Tiantian XU Tianpeng WU Zhaoxia JIN Yongjie LIU Yaqiang

Key Laboratory of Particle & Radiation Imaging (Tsinghua University), Ministry of Education, Department of Engineering Physics, Tsinghua University, Beijing 100084, China

Abstract The position decoding accuracy and the spatial resolution of positron emission tomography detectors are greatly influenced by the performance of the two-dimensional position map, including the gain uniformity of photomultiplier tube (PMT), the baseline offset of the PMT signals and the accuracy of analogue to digital converter (ADC). In this work, a PMT-quadrant sharing detector was designed. Two data acquisition platforms are employed to conduct the influence factors on the two-dimensional position map performances, one was that the waveforms of the PMT signals were scanned by the sequence acquisition mode based on the oscilloscope of LeCroy waveRunner 204MXi-A, and another was a self-developed high speed ADC data acquisition module. Results show that the event decoding positions were concentrated on the PMT with higher gain, the position map was distorted at the baseline offset of signal, and the cross-line artifacts were caused by the insufficient ADC sampling bit for a larger size position map. All the parameters need be adjusted properly to stabilize a real system, and the flexible oscilloscope platform can be used to design the detector block and the other platform with high ADC accuracy. Likely, the electrical circuit with a proper ADC accuracy adjusts the PMT gains and baseline offsets.

Key words PMT-quadrant-sharing, Two-dimensional position map, Gain uniformity, Baseline offset, Analogue to digital converter accuracy

1 Introduction

Position-sensitive scintillation detector blocks are widely used in positron emission tomography (PET), and are commonly designed as coupling the scintillation crystal array to four photomultiplier tubes (PMT) placed in the corners of the crystal array. Using the PMT-quadrant-sharing (PQS)[1–3], a traditional detector block can be improved in terms of cost and resolution, reducing 75% of the PMT number without sacrificing spatial resolution[1].

An incident gamma photon can generate thousands of optical photons in a scintillation crystal by its ionization interactions with the crystal material. The optical photons spreading in the detector block may reach the activity area of the four PMTs, and be converted to electronic signals, which can be used to determine position of the scintillation event by the Anger logic decoding methods. When the detector block is exposed to a uniform gamma source without collimation, the gamma photon events are recorded into a two-dimensional position map (2D map) by their positions detected. A crystal look-up table (CLT) is generated by segmenting the 2D map, defining the mapping between the position of a detected event and its incident crystal index. The 2D map quality is critical to the PET performance because mis-positioning of the gamma photon events causes image blurring, and reduces the spatial resolution[4–6].

Sharing of the optical photons affects the 2D map performances. The optical photon collection and

Supported by in part by Specialized Research Fund for the Doctoral Program of Higher Education (SRFDP200800031071), National Natural Science Foundation of China (No. 10975086), and the National High Technology Research and Development Program (863 Program) of China (No. 2006AA020802).

* Corresponding author. *E-mail address*: wangshi@mail.tsinghua.edu.cn

Received date: 2011-04-18

crystal decoding depend on the internal light- guide properties, such as crystal size, refractive index of the crystals and optical grease, number and nature of the interfaces, and the reflector patterns[7–11]. Also, factors affecting the 2D mapping performance include the gain uniformity of PMTs, baseline offset of PMT signals, and ADC accuracy. In this work, efforts were made against these electrical factors with two data acquisition platforms of an oscilloscope of LeCroy waveRunner 204MXi-A and a high speed ADC data acquisition module developed at our lab. The results showed that the event decoding positions would concentrate on the PMT of higher gain, the decoding map was distorted at the baseline offset of signal, and the cross-line artifacts were caused by insufficient ADC sampling bit for a larger size position map. The parameters should be adjusted properly to stabilize a real system. The oscilloscope platform is flexible and can be used to design the detector block and other platform with high ADC accuracy. The ADC of proper accuracy adjusts the PMT gains and baseline offsets.

2 Methods

2.1 Detector block design

The detector block with PQS scheme consists of a 6×6 yttrium orthosilicate (Y_2SiO_5, YSO) array coupled to four 19-mm XP1912 PMTs (Fig.1).

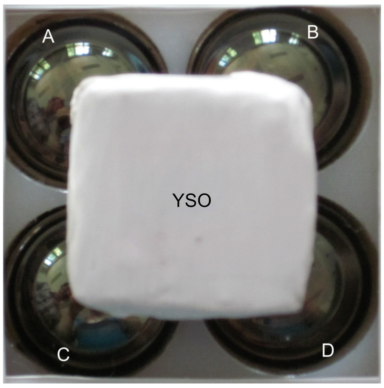

Fig.1 The crystal array (YSO), and the detector block with PQS scheme.

The crystals are of 3.18 mm ×3.18 mm × 20 mm in size and are coupled with reflectors (ESR, reflect ratio ≥98%) and optical grease (SAINT-GOBAIN BC-630). Each decoding position of scintillation event (X, Y) is calculated by Anger logic of the four PMT signals in Eq.(1).

$$\begin{aligned} &E=V_A+V_B+V_C+V_D \\ &E_X=V_B+V_D \\ &E_Y=V_A+V_B \\ &X=E_X/E \\ &Y=E_Y/E \end{aligned} \tag{1}$$

where, V_A, V_B, V_C, and V_D are the energy of four PMT signal. When a 2D map is measured and a CLT is generated, the (X,Y) value is used as an address to retrieve the index of the crystal pixel.

2.2 Oscilloscope-based data acquisition platform

The data acquisition platform based on the oscillo-scope of LeCory waveRunner 204MXi-A has 2- GHz bandwidth, 4 input channels in 10-GS/s of maximum sample rate, a 10 mCi ^{137}Cs γ-ray source, and a –1150 kV HV bias (Fig.2). The PMT signals are sent to relevant channels of the oscillo-scope, and summed in a front-end circuit to trigger the oscillo- scope.

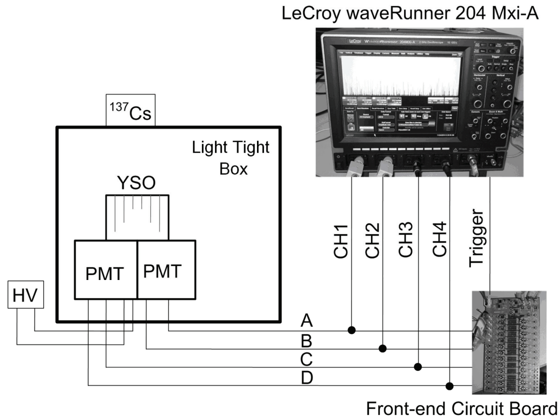

Fig.2 Schematics of the oscilloscope-based data acquisition platform.

The platform is flexible to record such information of the event waveforms as decay time constant of the scintillation and energy of PMT signals. The acquisition point under the sequence mode is 500 per waveform within the total acquisition time of 200 ns at the 0.4 ns/point, and 10 000 events in every 30 s are recorded, i.e. 400 000 gamma events can be acquired in 20 min, generating a 2D map with sufficient photon counts.

Figure 3 shows a representative waveform of PMT signals acquired by the oscilloscope. The signal energy was calculated by summing its 500 points. Fig.4(a) shows the calculated signal energies summed from 500 points for 370 000 events in the four PMTs that differ from each other in their gains and baseline offsets. One of the energies can be chosen as a reference signal for calibrating the other three energies by $V' = gain \times V + offset$, using nonlinear least squares fitting until the *gain* and *offset* are similar to those of the reference energy. Choosing PMT C as the reference signal, and adjusting its baseline offset to $V_C' = V_C + 1.00$, we obtained the fitting results as $V_A' = 1.85 \times V_A + 0.48$, $V_B' = 1.09 \times V_B + 0.90$, and $V_D' = 1.65 \times V_D + 1.78$, where V_A', V_B', V_C', and V_D' are the energy after the energy calibration (Fig.4b).

Because the crystals differ from each other in light collection, and the energy is not accurately determined by the oscilloscope, the photon-electrical peaks of the ^{137}Cs γ-ray of 662 keV are different in the total block.

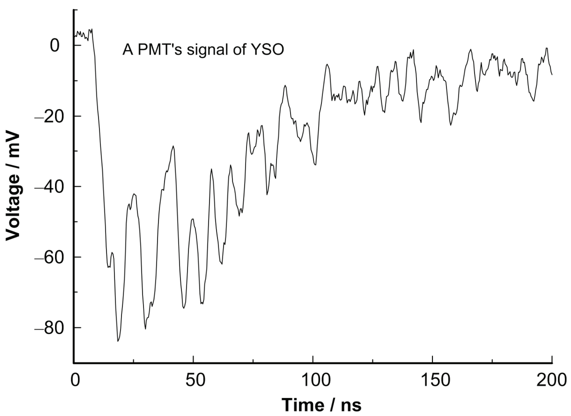

Fig.3 Waveform of PMT signal of YSO crystal at 500 point at 0.4 ns/point.

2.3 High speed ADC data acquisition platform

A high speed ADC data acquisition board was developed (Fig.5). The four signals are magnified, integrated in 200 ns, processed by Anger logic in analog hardware, and digitized by the 10-bit and 60 MHz ADC (ADS826). By setting each signal magnification ratio or the reference voltage, on the acquisition board one can adjust the gain or the baseline offset until a well 2D map is obtained. The output data are sent into the Power PC with a micro-control Linux system, from which the data were transited to the PC via a 100-M ethernet. The data acquisition terminal is developed by Labview 8.2[12].

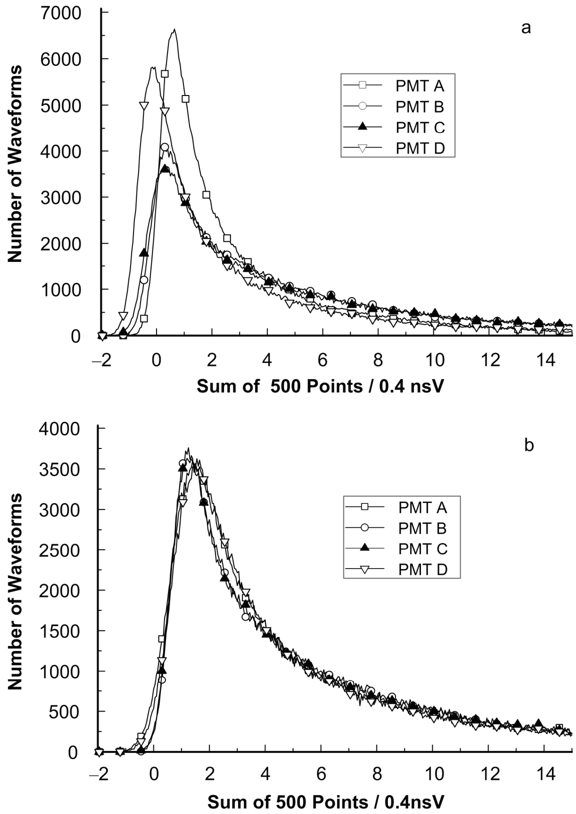

Fig.4 Signal energies of the four PMTs acquired by the oscilloscope (a), and the adjusted energies using PMT C as the reference(b).

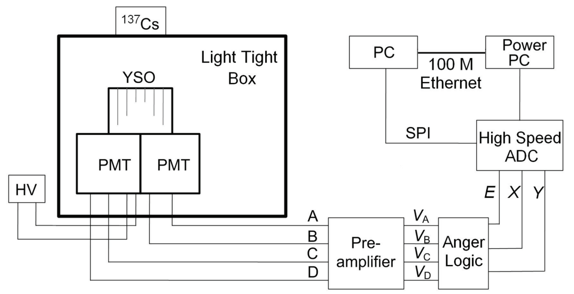

Fig.5 The platform of the high speed ADC acquisition board.

3 Results and Discussion

3.1 PMT gain adjustment

For an event, its decoding position (X, Y) calculated by Eq.(1) is $0 \le X \le 1$ and $0 \le Y \le 1$. The X and Y data are saved as the form of matrix. Fig.6 shows the processed waveform data acquired by the oscilloscope in a 128 × 128 matrix. Fig.6(a) is the 2D map with PMT gain properly adjusted ($V_A' = 1.85 \times V_A$, $V_B' = 1.09 \times V_B$, $V_C' = V_C$, $V_D' = 1.65 \times V_D$), and the 2D maps in Fig.6(b) and 6(c) are without the gain adjustments and the gain of PMT B over adjusted ($V_A' = 1.85 \times V_A$, $V_B' = 5 \times V_B$, $V_C' = V_C$, V_D'

$=1.65\times V_D$), respectively. The results show that changing the PMT gain results in big differences of the 2D maps. In Fig.6(c), over adjusting the gain of PMT B, the 2D map is the worst with slice-like decoding positions. In order to get a uniform distribution of the crystal response, the ability to adjust the PMT gains should be conducted by the detector system, and calibrated by gain-adjustable control circuitry, such as tunable PMT high voltage and variable gain amplifier[13].

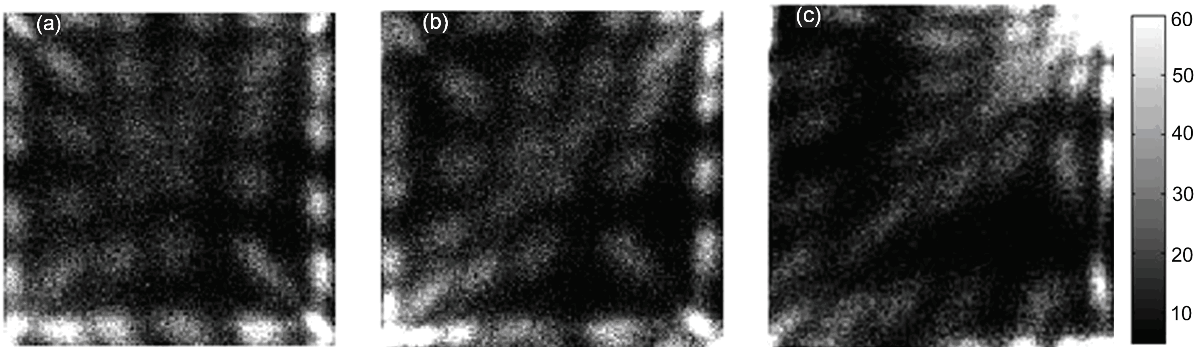

Fig.6 2D maps in a 128×128 matrix acquired by the oscilloscope with proper PMT gain adjustments (a), and without PMT gain adjustments (b) and the gain of PMT B over adjusted (c).

3.2 Baseline offset adjustment

The baseline offsets was adjusted by calibrating the PMT gain. In Fig.7(a), where $V_A'=1.85\times V_A+0.48$, $V_B'=1.09\times V_B+0.90$, $V_C'=V_C+1.00$, and $V_D'=1.65\times V_D+1.78$, as mentioned in Section 2.2, the 2D map is much better than that of Fig.6(a). With a –10-mV offset to PMT D, the decoding position moved out of the view of $0\leq X\leq 1$ and $0\leq Y\leq 1$ (Fig.7b), while with a +10-mV offset to PMT D, the decoding positions concentrated on PMT D (Fig.7c). In the system, the baseline offset is calibrated, automatically or manually, for the 2D map of central symmetry.

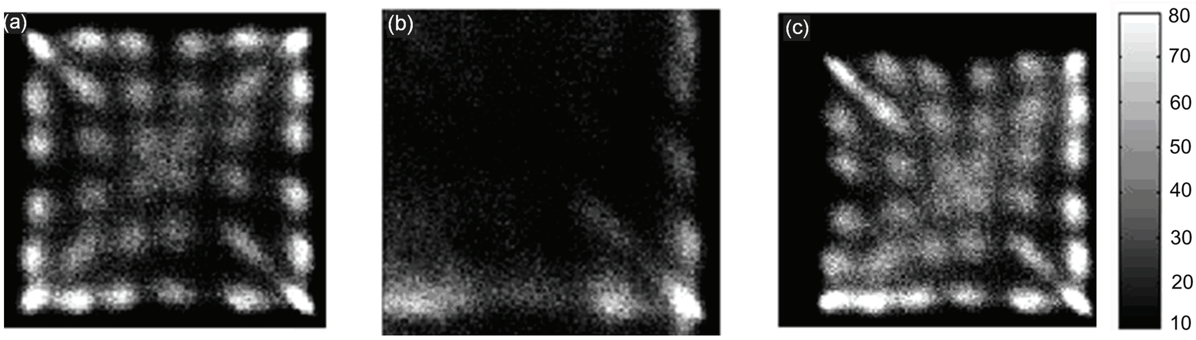

Fig.7 2D maps acquired by the oscilloscope with baseline offset accurately adjusted (a) and the PMT D baseline offset at –10 mV (b) and 10 mV(c).

3.3 ADC accuracy

The higher sampling accuracy of the ADC is, the more precise the measured energy is. The size of 2D map matrix is determined by the accuracy of ADC. The ADC for the oscilloscope-based platform is 8 bits, while the high speed ADC is 10 bits. After adjusting the PMT gain and calibrating the baseline offset with 0.4M events in 20 min, their 2D maps in 128×128 matrix acquired by the oscilloscope platform are shown in Fig.8(a) and 8(b), respectively, and the 2D map in 256×256 matrix acquired by the platform of high speed ADC using 10M events in 10 min is shown in Fig.8(c), which is of less noise and higher counting rate. The oscilloscope platform cannot record all the events because its writing memory is time-costly, but being capable of generating a fine 2D map in several minutes, it is flexible for designing the detector block.

The impact of ADC sampling bits was studied using the same data as Fig.8(c). The E_X, E_Y and E signals in 10 bits were re-sampled by $E_{X\mathrm{re}}=$ Floor($2^{-10}E_X\times 2^b$), $E_{Y\mathrm{re}}=$ Floor($2^{-10}E_Y\times 2^b$), and Eq.(2), $E_{\mathrm{re}}=$ Floor($2^{-10}E\times 2^b$), where the Floor function means rounding down to the nearest integer, and b is the ADC data bits. For ADC of 6, 7 and 8 data bits, the 2D maps are shown in Fig.9(a), 9(b) and 9(c). The 2D maps deteriorate in quality with decreasing ADC precision. The cross-line artifacts show that the poor energy determination affects the 2D map segmentation.

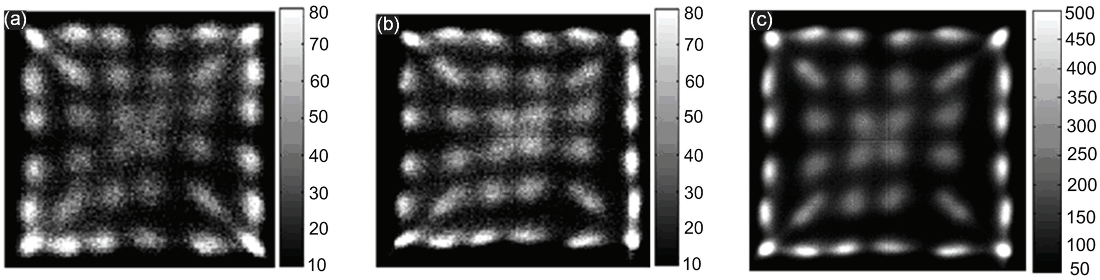

Fig.8 2D maps in 128×128 matrix using 0.4 M events in 10 min by oscilloscope (a) and the high speed ADC, (b), and the 256×256 2D maps using 10M in 20 min by the high speed ADC.

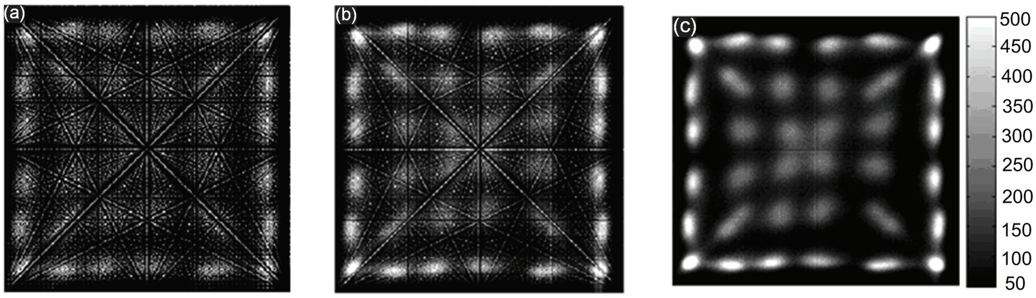

Fig.9 The 256×256 2D maps acquired with high speed ADC of (a) 6, (b) 7 and (c) 8 data bits.

For finding the factors causing the cross-line artifacts, one model was simplified with a series of integer data (E_X, E_Y, E), generating the pseudo 2D maps (p2D map), with E_X and E_Y being uniformly distributed between 1 and E. The p2D map with an approximate uniform distribution is shown in Fig.10 (a). However, if E is less than that of the p2D map matrix, some points of the p2D map have no counts. For example, if E=64 and the p2D map matrix is 256×256, the dynamic of E_X/E and E_Y/E would be [1/64, 2/64, 3/64 ... 64/64], and only 64×64 positions in the p2D map has the same counts (Fig.10b). When E is a range of number, more positions in the p2D map have the obvious non-uniform counts (Fig.10c). The position counts in the p2D map increases with the E range. However, some points have no counts, such as (3/256, 5/256), or bigger counts, such as (128/256, 128/256), because many Es with position counts in Fig.10(d) cause the cross-line artifacts. Some lines have larger counts, or no counts. So the cross-line artifacts are generated by a bit data of (E_X, E_Y, E), and drawn on a 2D map of bigger size.

So when the ADC of the data acquisition system is of high accuracy, the 8 bits for the 6×6 crystal array is acceptable. The ADC of good accuracy can be achieved with the crystal array of big size, such as 16 × 16. Moreover, the PMT gains should be set properly to ensure that the energy range of concern is in the dynamic voltage input of the ADC.

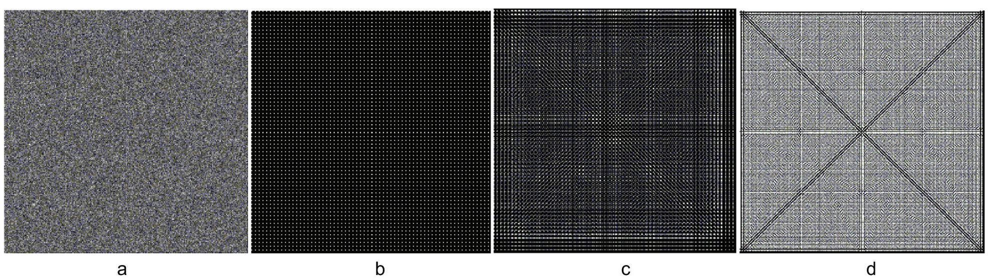

Fig.10 2D maps in 256×256 matrix with E_X=1–E and E_Y=1–E. (a) E=500–600, (b) E=64, (c) E=64–68, (d) E=64–100.

4 Conclusions

Two platforms of high speed ADC and the oscilloscope of LeCory waveRunner 204MXi-A were used to study the influence factors on 2D map performance of PET detector block of PQS design. The influence factors include the gain uniformity of PMTs, baseline offset of signals, and the ADC accuracy. The γ-ray events would concentrate on the PMT of higher gain. The decoding position is distorted at the signals of baseline offsets, and cross-line artifacts for a larger size 2D map are caused by insufficient ADC sampling bits. The oscilloscope can be used flexibly for designing detector block, and the platform with a proper ADC accuracy can adjust the PMT gains and baseline offsets, with stable performance of 2D map.

References

1 Wong W H. IEEE Trans Nucl Sci, 1993, **40:** 962–966.

2 Wong W H, Uribe J, Hicks K, *et al.* IEEE Trans Nucl Sci,1994, **41:** 1453–1457.

3 Wong W H, Uribe J, Hicks K, *et al.* IEEE Trans Nucl Sci, 1995, **42:** 1095–1101.

4 Kang X, Gu Z, Sun X, *et al.* Comparing crystal identification algorithms for PET block detectors. IEEE NSS/MIC Conference Record. Dresden, Germany. Oct. 2008, 4562–4566.

5 Kang X, Liu Y, Jin Y, *et al.* A new module-level parameter interfusion ratio (IR) to evaluate the performance of PET detector block. IEEE NSS/MIC Conference Record. Knoxville, USA, Otc. 2010.

6 Aykac M, Li H, Uribe J, *et al.* IEEE Trans Nucl Sci, **50:** 1331–1338.

7 Ramirez R A, Liu S, Liu J, *et al.* IEEE Trans Nucl Sci, 2008, **55:** 862–869.

8 Li H, Wong W H, Kim S, *et al.* IEEE Trans Nucl Sci, 2006, **53:** 2557–2562.

9 Liu S, Li H, Zhang Y, *et al.* IEEE Trans Nucl Sci, 2009, **56:** 2614–2620.

10 Janecek M, Moses W W. IEEE Trans Nucl Sci, 2010, **57:** 964–970.

11 Wei Q, Liu Y, Ma T, *et al.* Monte Carlo studies on a novel PET block detector design scheme with cross-shape PMT layout. IEEE NSS/MIC Conference. Record, 2010.

12 Kang X, Liu Y, Sun X, *et al.* A fast accuracy crystal identification method based on fuzzy C-means (FCM) clustering algorithm for MicroPET. IEEE BMEI Conference. Record, San Ya, China. Oct. 2008, 779–782.

13 Wang Y, Wong W H, Aykac M, *et al.* IEEE Trans Nucl Sci, 2002, **49:** 2047–2050.